PROCEEDINGS OF SCIENCE

Ultraheavy Nuclei as Ultrahigh-Energy Cosmic Rays: Constraints from Collapsars and neutron star mergers

B. Theodore Zhang[1], **Kohta Murase**[2,3,4,1], **Nick Ekanger**[5], **Mukul Bhattacharya**[2,3,4], **Shunsaku Horiuchi**[5,6]

[1]*Center for Gravitational Physics and Quantum Information, Yukawa Institute for Theoretical Physics, Kyoto University, Kyoto, Kyoto 606-8502, Japan*

[2]*Department of Physics, The Pennsylvania State University, University Park, PA 16802, USA*

[3]*Department of Astronomy & Astrophysics, The Pennsylvania State University, University Park, PA 16802, USA*

[4]*Center for Multimessenger Astrophysics, Institute for Gravitation and the Cosmos, The Pennsylvania State University, University Park, PA 16802, USA*

[5]*Center for Neutrino Physics, Department of Physics, Virginia Tech, Blacksburg, VA 24061, USA*

[6]*Kavli IPMU (WPI), UTIAS, The University of Tokyo, Kashiwa, Chiba 277-8583, Japan*

E-mail: zhangbing@ihep.ac.cn

We investigate the propagation of ultraheavy (UH) nuclei as ultrahigh-energy cosmic rays (UHECRs). We show that their energy loss lengths at $\lesssim$ 300 EeV are significantly longer than those of protons and intermediate-mass nuclei, and that the highest-energy cosmic rays with energies beyond $\sim$ 100 EeV, may originate from such UH-UHECRs. We derive constraints on the contribution of UH-UHECR sources, and the allowed energy generation rate densities are consistent with those of collapsars and compact binary mergers. A nearby transient, e.g., a low-luminosity gamma-ray bursts (LL GRBs), may give a special contribution to the observed UHECR flux, and we explore the possibility of simultaneously explaining both the Auger and TA spectra. These models predict a measurable shift toward heavier compositions above 100 EeV, testable with next-generation UHECR observatories.

39th International Cosmic Ray Conference (ICRC2025)
15–24 July 2025
Geneva, Switzerland

PoS(ICRC2025)445

1. Introduction

The origin of ultrahigh-energy cosmic rays (UHECRs) has been a long-standing mystery for over 50 years since the first detection of $\sim$ 100 EeV cosmic rays. The origin of UHECRs remains one of the most significant unresolved problems in modern astroparticle physics. Since their first detection in the 1960s, substantial progress has been made in measuring their energy spectrum.

Traditionally, there are two basic requirements of UHECR sources, Hillas condition and energetics of UHECRs. The total energy generation density of the UHECRs above $\sim$ 3 EeV, as inferred from the observations, is $Q_{\rm inj} \sim 6 \times 10^{44}$ erg Mpc^{-3} yr^{-1} for mixed composition [1]. The Hillas condition is often considered a confinement condition, representing the maximum acceleration capability of a source. Various sources meet this condition, making them potential candidates for UHECRs.

There are new clues for the sources of UHECRs from latest observations by Auger and TA, including composition and anisotropy. The large-scale anisotropy of UHECRs, particularly the dipole observed by the Auger Collaboration, provides strong evidence that UHECRs originate from extragalactic sources [2]. Auger data suggest a mixed composition of UHECRs, with intermediate-mass nuclei(e.g., carbon and oxygen) and/or heavy nuclei (e.g., iron) contributing significantly beyond 10 EeV [3]. In particular, the fraction of protons gradually decreases above the ankle, while intermediate-mass nuclei may become dominant at higher energies. The contribution of heavy nuclei appears negligible in the energy range of $10^{18.4}$ – $10^{19.4}$ eV [3], but these results are strongly influenced by hadronic interaction models. The distribution of $X_{\rm max}$, measured by TA, is consistent with Auger data, although the interpretation is still debated. Recent analysis suggests narrow rigidity and nearly identical sources, with a factor of two dispersion in maximum rigidity [4].

In recent years, there has been a surge in the detection of transient high-energy sources across the entire electromagnetic spectrum, from radio to gamma rays. Transient sources that are linked to the deaths of massive stars, including gamma-ray bursts (GRBs), engine-driven supernova/hypernova, pulsars, and magnetar-driven transients. GRBs are the brightest and probably the most powerful high-energy astrophysical phenomenon in the Universe. High-luminosity GRBs (HL GRBs) have typical isotropic radiation luminosity $\sim 10^{51}$ – 10^{53} erg s^{-1}. GRBs are treated as promising sources of UHECRs due to their acceleration ability and energetics. Unlike high-luminosity (HL) GRBs, low-luminosity (LL) GRBs allow nuclei to survive, the narrow-rigidity problem could be solved if the external shock accelerates the CRs, and the event rate of LL GRBs is higher than that of HL GRBs [5]. New-born pulsars and magnetars are formed following the massive stellar collapse and low-mass neutron star merger remnant. Heavy nuclei may come from the neutron star's surface and accelerate to the UHE energy range. Tidal disruption events (TDEs) have been suggested as the sources of UHECRs [6]. A fraction of TDEs have relativistic jets, e.g., Sw J1644, Sw J2058, Sw J1112, and AT 2022cmc. UHECRs could be accelerated in the internal and external reverse/forward shock of TDE jets [6].

2. Ultraheavy nuclei

Ultraheavy (UH) nuclei, which are defined as nuclei heavier than iron-group nuclei throughout this work, are believed to be synthesized due to the r-process occurring inside neutron-rich envi-

ronments . The sources of UH nuclei can be BNS and neutron-star–black-hole (NSBH) mergers, as well as collapsars including GRBs and magnetorotational supernovae.

Compact binary mergers include binary neutron star mergers (NS-NS) and black hole-neutron star mergers (BH-NS). Short GRBs are often associated with NS-NS and BH-NS mergers, their jets are efficient acceleration sites of CRs as long GRBs. For merger shocks, the large charge number can accelerate ultra-heavy UHECR (UH-UHECR) nuclei to the UHE energy range. UH nuclei are synthesized as a result of the r-process occurring inside neutron-rich environments. The third peak material exists in the equatorial plane (dynamical ejecta). Merger shocks from NS-NS or BH-NS mergers have been suggested to the sources of UH-UHECR nuclei, which could be associated with the origin of the Amaterasu particle [7, 8].

UH nuclei synthesized in magnetically dominated GRB outflows are discussed as UHECRs, and possible signatures of UHECR nuclei are investigated. UH nuclei have the advantage of being accelerated to energies beyond 100 EeV, compared to conventional light- and intermediate-mass group nuclei, which could provide an additional contribution to the highest-energy CRs.

3. Propagation of Ultraheavy nuclei

UH nuclei can be photodisintegrated and spalled into lighter nuclei due to their interactions with background target photons and matter, respectively. For the propagation of UHECRs from their source to Earth, interactions with the cosmic microwave background (CMB) and extragalactic background light (EBL) are dominant, and we utilize the public code CRPropa 3.2 to propagate UHECRs through intergalactic space [9]. However, because CRPropa 3.2 does not provide a module for nuclei with mass numbers of $A > 56$, we newly generate the photodisintegration cross section table of UH-UHECRs using the nuclear reaction network Talys 1.96 [10, 11] as an extension to CRPropa 3.2. In our photodisintegration reaction network, the maximum atomic number and mass number of nuclei are $Z = 92$ and $A = 238$, respectively, with a total of 2434 isotopes. In addition, the decay of unstable UH-UHECRs is implemented with the data table taken from NuDat 3 [12].

The survival of nuclei is one of the main arguments for finding the sources of UHECRs. We can estimate the energy loss time scale using the following formula

$$t_{A\gamma}^{-1}(E_A) = \frac{c}{2\gamma_A^2}\int_{\bar{\varepsilon}_{\rm th}}^{\infty} d\bar{\varepsilon}\sigma_{A\gamma}(\bar{\varepsilon})\kappa_A(\bar{\varepsilon})\bar{\varepsilon}\int_{\bar{\varepsilon}/2\gamma_A}^{\infty} d\varepsilon\frac{1}{\varepsilon^2}\frac{dn}{d\varepsilon}, \tag{1}$$

where γ_A is the Lorentz factor of UHECRs with the mass number A, $\varepsilon_{\rm th}$ is the threshold energy measured in the rest frame of the initial nucleus (NRF) and $\mathrm{d}n/\mathrm{d}\varepsilon$ is the differential number density of target photons [6]. Here, $\sigma_{A\gamma}(\bar{\varepsilon}) = A\sigma_{p\gamma}(\bar{\varepsilon})$ is the photohadronic cross-section related to the photomeson or photodisintegration process. The inelasticity is $\kappa_{A\gamma}(\bar{\varepsilon}) \equiv \frac{\Delta E}{E} = \frac{\Delta N}{N}$, where N is the total number of nucleons in the parent nuclei, and ΔN is the number of ejected nucleons in each channel. The inverse of the total energy loss length is written as $\lambda_{\rm loss}^{-1} = \lambda_{\rm loss,phdis}^{-1} + \lambda_{\rm loss,phmes}^{-1} + \lambda_{\rm loss,BH}^{-1} + \lambda_{\rm loss,ad}^{-1}$, where $\lambda_{\rm loss,ad} = c/H_0 \sim 4000$ Mpc is the adiabatic energy loss length. The photodisintegration energy loss length is $\lambda_{\rm loss}^{\rm phdis} \approx \left(n_{\rm CMB}\hat{\sigma}_{\rm phdis}\right)^{-1} \simeq 1.3(A/195)^{-0.21}$ Mpc, where $\hat{\sigma}_{\rm dis} = \sigma_{A\gamma}\kappa_{A\gamma}$ is the effective photodisintegration cross section and $\kappa_{A\gamma} \approx 1/A$ is the inelasticity at the giant dipole resonance (GDR). The effective photodisintegration cross section for UH nuclei can be analytically approximated as $\sigma_{A\gamma} \approx \sigma_{\rm GDR}\Delta\bar{\varepsilon}_{\rm GDR}/\bar{\varepsilon}_{\rm GDR} \approx 120(A/195)^{1.21}$ mb for $A \gtrsim 10$, where

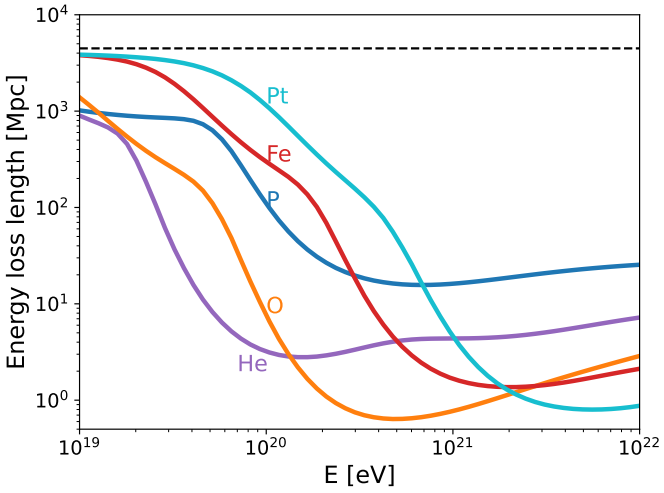

Figure 1: Total energy loss lengths for various nuclei: p, He, O, Fe, and Pt. The black dashed line is the energy loss length due to the adiabatic expansion of the universe. CMB and EBL are considered as target photons.

$\sigma_{\rm GDR} \approx 4.3\times10^{-28}A^{1.35}$ cm^2 is the GDR cross section, $\Delta\bar{\varepsilon}_{\rm GDR} \approx 21.05A^{-0.35}$ MeV is the width, and $\bar{\varepsilon}_{\rm GDR} \approx 42.65A^{-0.21}$ MeV is the resonance energy in the nuclear rest frame. The typical resonance energy is $E_A^{\rm phdis} \approx 0.5Am_pc^2\bar{\varepsilon}_{\rm GDR}/\varepsilon_t \simeq 1.9\times10^{21}$ eV $(A/195)^{0.79}(\varepsilon_t/6.6\times10^{-4}$ eV$)^{-1}$, where ε_t is the target photon energy. Extrabackground light (EBL) is more relevant to the photodisintegration of UH nuclei with $\sim 10^{20}$ eV. Energy losses due to the Bethe-Heitler pair production process are also important for UH-UHECRs because of their large atomic numbers. The photomeson production process is irrelevant when considering the propagation of UH-UHECRs due to the high-energy threshold at $\sim 4\times10^{22}$ eV $(A/195)(\varepsilon_t/6.6\times10^{-4}$ eV$)^{-1}$. As seen in Fig 1, UH-UHECRs can travel longer distances than the GZK (Greisen-Zatsepin-Kuzmin) distance for UHECR protons and the energy loss length of iron-group-mass nuclei.

To calculate the UHECR spectrum and composition on Earth, we take into account the change in the composition of UH-UHECRs during propagation, as the UH nuclei become progressively lighter with the ejection of one or more nucleons. In Fig. 2, we provide the results of our fitting for the energy spectrum and composition of UHECRs measured by Auger. We see that the energy generation rate density of the three UH nuclear species is constrained to be $Q^{\rm Auger}_{\rm UH-UHECR} \lesssim (0.1-15)\times10^{42}$ erg Mpc^{-3} yr^{-1}. The results for the TA data are shown in Fig. 2, where we find that the energy generation rate densities of UH-UHECRs are constrained to be $Q^{\rm TA}_{\rm UH-UHECR} \lesssim (1.4-5.6)\times10^{43}$ erg Mpc^{-3} yr^{-1}, for both composition models, which is about 3 times larger than that derived based on the Auger data for both composition models.

4. Origin of Amaterasu particle

Recently, TA detected an Amaterasu particle with an energy of $E = 240$ EeV, the second highest energy cosmic ray detected on Earth [18]. The highest energy UHECR, at 320 EeV, was detected by the Fly's Eye air shower detector in 1991. However, no clear sources have been identified

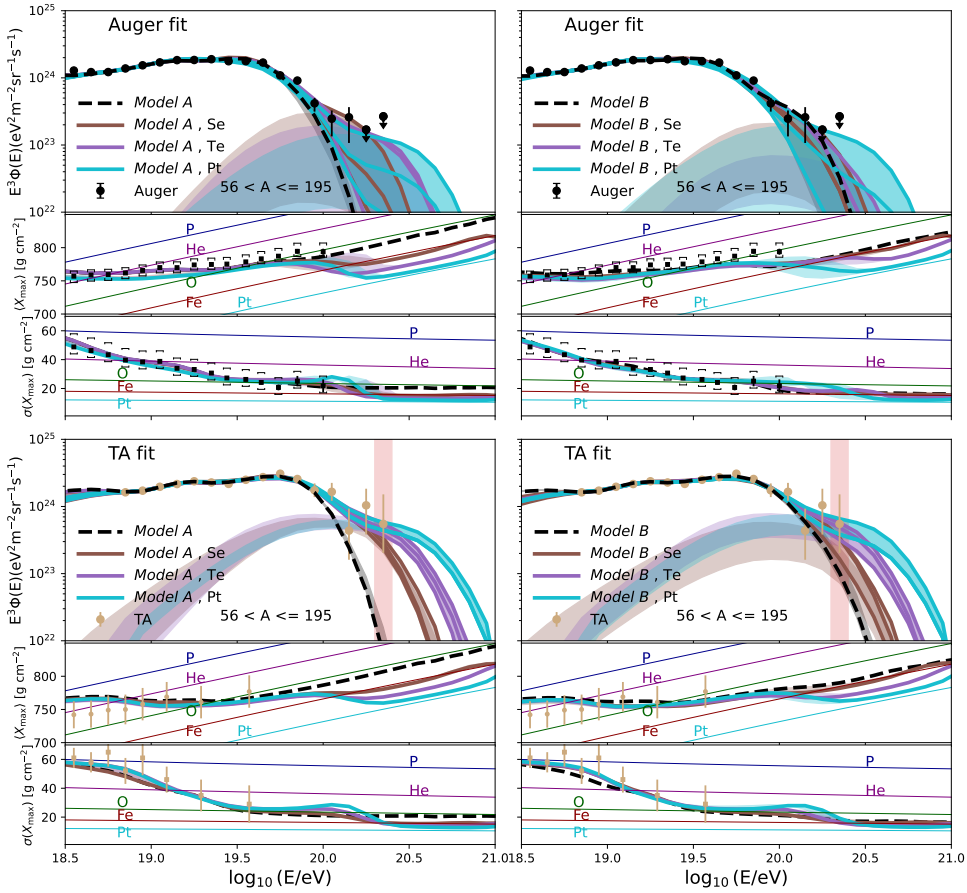

Figure 2: Energy spectra and the first/second moments of $X_{\rm max}$ distribution are shown considering both conventional and UH nuclei. Auger data are obtained from Refs. [13, 14], while TA data are from Refs. [15, 16]. Note that the data point in the red vertical band corresponds to the Amaterasu particle [17].

for these highest-energy CRs. As shown in Fig. 2, the Amaterasu particle may be explained as a UH-UHECR event.

To explore this possibility in more detail, we examine the backtracked direction of the Amaterasu particle for different nuclear species, as shown in Fig. 3, where we adopt the Galactic magnetic field model. For light or even iron nuclei, the direction of the Amaterasu particle lies in the local void region (yellow dotted curve in Fig. 3). If it is a UH nucleus, the source may exist outside the local void or even near the supergalactic plane thanks to the larger atomic number.

5. Possible contribution from a nearby transient

Based on the best-fit model to the Auger data, we assume there are some nearby transient sources in the northern sky, mainly coming from the supergalactic plane, accounting for the spectral

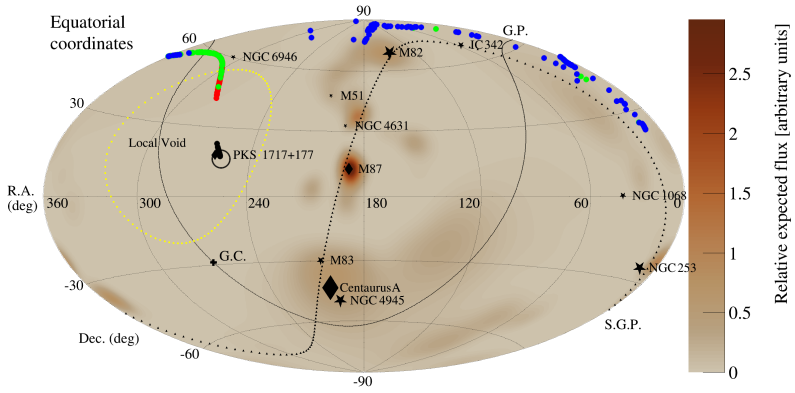

Figure 3: Skymap of backtracked particles with mean energy $E = 244$ EeV and variation $E = 70$ EeV for p ($Z = 1$, black), Fe ($Z = 26$, red), Zr ($Z = 40$, green) and Pt ($Z = 78$, blue) in equatorial coordinates. For each nuclear species, we inject 100 particles. The arrival direction of the Amaterasu particle is (R.A., Dec.) = $(255.9 \pm 0.6^\circ, 16.1 \pm 0.5^\circ)$ in equatorial coordinates, indicated as a black circle. The black circle indicates the arrival direction of the Amaterasu particle. The supergalactic plane (S.G.P.) is shown as black dotted curves, and the Galactic plane (G.P.) is shown as black solid curves. The color bar represents the expected relative flux from sources in the local large-scale structure.

excess observed by TA . We show a specific example in Fig. 4, where the flux per steradian is calculated by dividing the total flux by the detector's field of view, $\Delta\Omega \sim 2\pi$. The observed TA spectral excess may be affected by the systematic uncertainty on the energy scale, and we decrease the TA energy scale by a factor of 8.5% to match the Auger spectra in the low-energy range.

Based on the best-fit model to the Auger data, we assume there are some nearby transient sources in the northern sky, mainly coming from the supergalactic plane, accounting for the spectral excess observed by TA. For demonstrative purposes, we assume a nearby low-luminosity GRB located at $d = 5$ Mpc from Earth, and adopt the 16TJ model shown in Table I of Ref. [5] as the default composition model of nuclei, $f_{\rm O} : f_{\rm Si} : f_S = 0.52 : 0.37 : 0.11$, and the total injection UHECR luminosity above 10^{18} eV is $\mathcal{L}_{\rm UHECR} \simeq 0.7 \times 10^{41}$ erg s^{-1}. Additionally, UH nuclei could be synthesized in the relativistic jet of GRBs, where the most abundant UH nuclei can be the first-peak r-process elements such as Se, and the corresponding injection luminosity is $\mathcal{L}_{\rm UH-UHECR} \simeq 0.7 \times 10^{40}$ erg s^{-1}. The typical delay time of UHECRs by the extragalactic magnetic field can be $\tau_d^{\rm EG} \sim 1.7$ yr $(Z/34)^2 E_{\rm A,20.5}^{-2} B_{\rm EG,-11.5}^2 (l_c/1\,{\rm Mpc})(d/5\,{\rm Mpc})$, where $B_{\rm EG}$ is the magnetic field strength that can be very weak in the void region, and d is source distance. The Galatic magnetic field cause an inevitable time delay, $\tau_d^{\rm Gal} \sim 200$ yr for a particle with rigidity 5 EV. Thus, the total required energy of UHECRs emitted by a transient source is estimated to be $\mathcal{E}_{\rm UHECR} \sim (\mathcal{L}_{\rm UHECR} + \mathcal{L}_{\rm UH-UHECR})(\tau_d^{\rm EG} + \tau_d^{\rm Gal}) \simeq 4.5 \times 10^{50}$ erg, which can be consistent with cosmic-ray energy budgets of collapsars. Note that even in this specific case our constraints on the energy generation rate density of UH-UHECRs still hold, and the results with the Auger data are applicable.

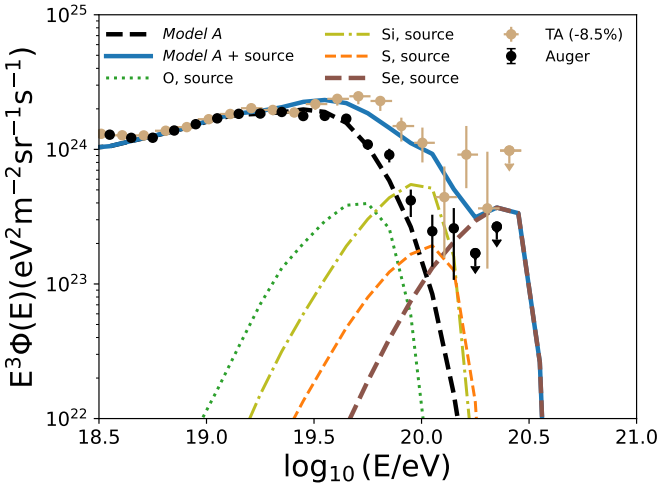

Figure 4: Demonstrative example for explaining the TA spectrum with the best-fit model to the Auger data (*Model A*) with an additional contribution of UHECRs including UH nuclei from collapsars.

6. Summary

We provided detailed study on the propagation of UH-UHECRs, and derived general constraints on their contribution to the observed UHECR flux. Thanks to their energy loss lengths at $\lesssim 10^{21}$ eV, which are longer than those of protons and intermediate-mass nuclei, UH-UHECRs may significantly contribute to the highest-energy cosmic rays beyond $\sim 10^{20}$ eV, including the Amaterasu event. The allowed energy generation rate densities are consistent with those of collapsars and compact binary mergers.

References

[1] Alexander Aab et al. Features of the Energy Spectrum of Cosmic Rays above 2.5×10^{18} eV Using the Pierre Auger Observatory. *Phys. Rev. Lett.*, 125(12):121106, 2020.

[2] Alexander Aab et al. Observation of a Large-scale Anisotropy in the Arrival Directions of Cosmic Rays above 8×10^{18} eV. *Science*, 357(6537):1266–1270, 2017.

[3] Adila Abdul Halim et al. Studies of the mass composition of cosmic rays and proton-proton interaction cross-sections at ultra-high energies with the Pierre Auger Observatory. *PoS*, ICRC2023:438, 2023.

[4] Domenik Ehlert, Foteini Oikonomou, and Michael Unger. Curious case of the maximum rigidity distribution of cosmic-ray accelerators. *Phys. Rev. D*, 107(10):103045, 2023.

[5] B. Theodore Zhang, Kohta Murase, Shigeo S. Kimura, Shunsaku Horiuchi, and Peter Mészáros. Low-luminosity gamma-ray bursts as the sources of ultrahigh-energy cosmic ray nuclei. *Phys. Rev.*, D97:083010, 2018.

[6] B. Theodore Zhang, Kohta Murase, Foteini Oikonomou, and Zhuo Li. High-energy cosmic ray nuclei from tidal disruption events: Origin, survival, and implications. *Phys. Rev.*, D96(6):063007, 2017.

[7] B. Theodore Zhang, Kohta Murase, Nick Ekanger, Mukul Bhattacharya, and Shunsaku Horiuchi. Ultraheavy Ultrahigh-Energy Cosmic Rays. 5 2024.

[8] Glennys R. Farrar. Binary neutron star mergers as the source of the highest energy cosmic rays, 5 2024.

[9] Rafael Alves Batista et al. CRPropa 3.2 — an advanced framework for high-energy particle propagation in extragalactic and galactic spaces. *JCAP*, 09:035, 2022.

[10] A. J. Koning, S. Hilaire, and M. C. Duijvestijn. TALYS: Comprehensive Nuclear Reaction Modeling. *AIP Conf. Proc.*, 769(1):1154, 2005.

[11] Koning, A. J., Hilaire, S., and Duijvestijn, M. C. TALYS-1.0. *International Conference on Nuclear Data for Science and Technology*, pages 211–214, 2007.

[12] NuDat 3 Data Base, National Nuclear Data Center (NNDC), Brookhaven National Laboratory, Upton, NY, USA. https://www.nndc.bnl.gov/nudat3/.

[13] Alexander Aab et al. Measurement of the cosmic-ray energy spectrum above 2.5×10^{18} eV using the Pierre Auger Observatory. *Phys. Rev. D*, 102(6):062005, 2020.

[14] A. Abdul Halim et al. Inference of the Mass Composition of Cosmic Rays with energies from $\mathbf{10^{18.5}}$ to $\mathbf{10^{20}}$ eV using the Pierre Auger Observatory and Deep Learning, 6 2024.

[15] R. U. Abbasi et al. Observation of Declination Dependence in the Cosmic Ray Energy Spectrum, 6 2024.

[16] R. U. Abbasi et al. Depth of Ultra High Energy Cosmic Ray Induced Air Shower Maxima Measured by the Telescope Array Black Rock and Long Ridge FADC Fluorescence Detectors and Surface Array in Hybrid Mode. *Astrophys. J.*, 858(2):76, 2018.

[17] R. U. Abbasi et al. An extremely energetic cosmic ray observed by a surface detector array. *Science*, 382(6673):abo5095, 2023.

[18] Jihyun Kim et al. Highlights from the Telescope Array Experiment. *PoS*, ICRC2023:008, 2024.

PoS(ICRC2025)445